Saturable nonlinear refraction in hot atomic vapor

C. F. McCormick, D. R. Solli, and R. Y. Chiao
Department of Physics, UC Berkeley, Berkeley, California 94720-7300, USA

J. M. Hickmann*
Departamento de Física, Universidade Federal de Alagoas, Cidade Universitária, 57072-970, Maceió, Alagoas, Brazil
and Department of Physics, UC Berkeley, Berkeley, California 94720-7300, USA

(Received 16 September 2003; published 12 February 2004)

Atomic vapors make flexible and useful nonlinear optical media when light is detuned far from resonances. However, few direct measurements of their nonlinear coefficients have been performed to date. We present a measurement of the Kerr coefficient for various detunings to both the red and blue of the $D2$ line in hot atomic rubidium vapor. Saturation effects complicate the interpretation of the standard z-scan method, but a simple saturation model agrees well with our data. We find values of $n_2 \approx \pm 10^{-7}$ cm^2/W for 1 GHz detunings from the $D2$ line.

DOI: 10.1103/PhysRevA.69.023804 PACS number(s): 42.65.Jx, 42.65.Hw, 32.10.−f

Nonlinear optics in atomic vapors has a rich history. A variety of nonlinear effects has been observed in hot atomic gases, including self-focusing [1], self-trapping [2], self-bending [3], four-wave mixing [4], and beam waveguiding [5,6]. Atomic vapors have a resonant nonlinearity, arising from two-level absorption. While inhomogeneous Doppler broadening complicates the atomic response [7,8], for large Doppler widths the system is well-understood theoretically. However, to date few clean measurements of the Kerr coefficient for these systems have been made [9,10]. We present here a direct measurement of the Kerr coefficient n_2 for far-detuned atomic rubidium, discussing the role of saturation in the measurements and comparing two simple models for the frequency dependence of the nonlinearity.

Our experimental tool is based on the z-scan method, a well-established technique for measuring Kerr coefficients [11,12]. A focused Gaussian beam is passed through a thin sample (compared to the Rayleigh range) of the material being studied, and is detected in the far field through an on-axis aperture. Self-focusing or -defocusing caused by the medium changes the far-field beam size and is detected by the change of light intensity through the aperture. By scanning the sample along the propagation (z) axis, the Kerr coefficient can be extracted from the overall transmission curve against longitudinal position. The sign of the nonlinearity is obtained from the symmetry of the scan.

The standard equation for the Kerr coefficient of an atomic vapor is derived by taking the limit of low intensity in the expression for the index of refraction in a two-level atomic system. For large detunings and using the convention $n(I)=n_0+n_2 I$ one obtains [1,13]

$$n_2(\mathrm{cm}^2/\mathrm{W}) = 10^4 \times \frac{\mu_{12}^4 N}{2c\epsilon_0^2 h^3 \delta^3}, \qquad (1)$$

where μ_{12} is the dipole matrix element, N is the number density of atoms, and $\delta=\nu-\nu_0$ is the detuning from resonance. The dependence on $1/\delta^3$ makes n_2 antisymmetric in detuning and variable in size. For the $D2$ transition of rubidium vapor at 78 °C, $\mu_{12}=2.52\times10^{-29}$ C m, $N=10^{18}$ m^{-3}, and a detuning of $+1.0$ GHz gives a theoretical Kerr index $n_2=2.9\times10^{-7}$ cm^2/W.

This expression appears frequently in the literature and is taken somewhat on faith by many workers. Various models including more levels have been proposed to explain cross-phase effects from other electric fields [5,6,14], but these models are generally not necessary to explain self-effects [8]. However, Eq. (1) is valid only for a gas in which homogeneous broadening dominates. For atomic vapors at or above room temperature, a more accurate approach is to begin with the expression for the inhomogeneously (Doppler-) broadened index of refraction [7,8] and take the limit of low intensity, which gives

$$n_2(\mathrm{cm}^2/\mathrm{W}) = 10^4 \times \frac{4\pi^{7/2}}{3} \frac{\mu_{12}^4 N}{c\epsilon_0^2 h^3} \left(\frac{T_2}{k^2 u^2}\right) x e^{-x^2}, \qquad (2)$$

where T_2 is the dephasing time of the atomic transition ($=2T_1$ in the absence of collisions, a reasonable assumption here), k is the momentum of the incident light, $u=\sqrt{2k_B T/M}$ is the width of the atomic velocity distribution, and $x \equiv 2\pi\delta/ku$. Note that n_2 is still antisymmetric in this expression but has a different dependence on detuning than in Eq. (1). For the same atomic density as above, a detuning of $+1.0$ GHz gives $n_2=1.4\times10^{-7}$ cm^2/W. This "Doppler" form of n_2 is only valid in the limit of large Doppler broadening compared to the homogenous linewidth, but this is generally the case for alkali vapors at room temperature or higher.

An important but counterintuitive point to be made about atomic vapors as nonlinear media is that they are extremely easy to saturate. Unlike crystalline optical media which require mode-locked lasers to display appreciable nonlinear effects, the saturation intensity of atomic vapors at zero detuning is of the order of milliwatts per square centimeter. This makes it possible to observe nonlinear optical phenom-

*Electronic address: hickmann@loqnl.ufal.br

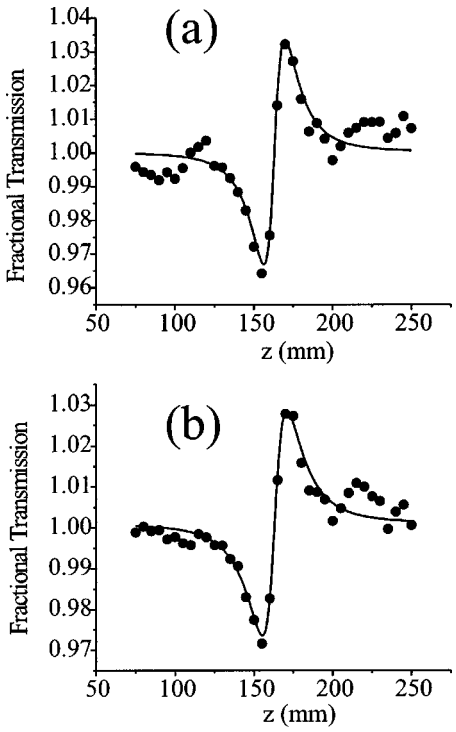

FIG. 1. Sample z scan data for scans to the blue of the ^{85}Rb $F=3\rightarrow F'$ transition. (a) $\delta=0.8$ GHz, input power 1.0 mW; (b) $\delta=1.1$ GHz, input power 5.0 mW. Fit is to Eq. (3).

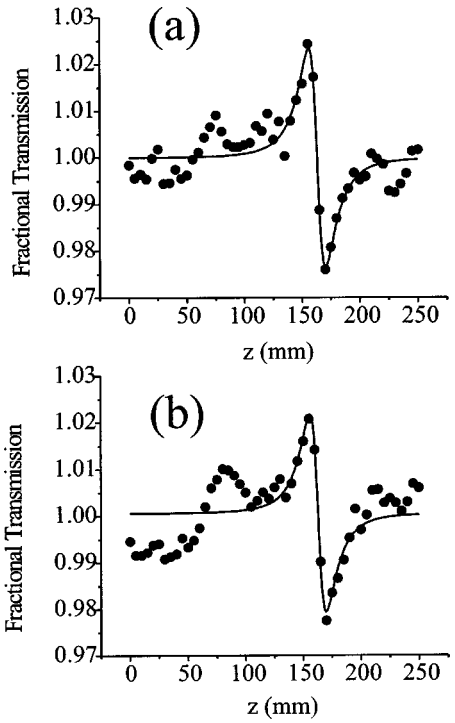

FIG. 2. Sample z scan data for scans to the red of the ^{87}Rb $F=2\rightarrow F'$ transition. Note the fringe effect at low-z values. (a) $\delta=0.9$ GHz, input power 6.0 mW; (b) $\delta=1.1$ GHz, input power 8.0 mW. Fit is to Eq. (3).

ena with low-intensity continuous wave (CW) lasers, but also means that saturation effects must be considered unless the incident beam intensities are kept extremely small.

We performed a series of z-scan measurements on hot (78 °C), natural-abundance rubidium (72% ^{85}Rb, 28% ^{87}Rb) vapor with light at various detunings from the $D2$ line. Our detunings were chosen so as to make linear and nonlinear absorption negligible while still observing an appreciable nonlinear refractive effect.

The z-scan beam in our experiment was provided by a tunable CW titanium-sapphire (Ti:sapphire) laser with a roughly 10 MHz bandwidth. The light was first spatially filtered through a 30 μm hole and then focused through a lens ($f=250$ mm) to produce a nearly Gaussian beam with a estimated Rayleigh range (z_R) around 6 mm. In the far field, the beam was detected by a large area photodetector, in front of which was placed an aperture with 2.5% linear fluency, centered on the beam. To improve the signal to noise ratio, a chopping wheel rotating at 225 Hz cut the beam before the spatial filter and the photodetector signal was fed into a lock-in amplifier.

In order to determine the detuning from the resonance, a small fraction of the beam was interfered on a fast photodiode with light from an independent diode laser locked to the Rb transition using saturated absorption spectroscopy. The resulting beat note signal was fed into a digital oscilloscope which performed a real-time fast Fourier transform on it. This method allowed us to monitor the laser detuning with a precision of about 20 MHz over a range of ± 2 GHz of the locking transition. The frequency of the Ti:sapphire laser was stableover periods of time longer than the time scale of the scans (approximately 2 min).

We placed a vapor cell filled with natural-abundance rubidium in the beam path after the lens. The cell was thin compared to the Rayleigh range ($L=1$ mm) and was tilted at 30° to reduce interference effects from multiple reflections in the cell's walls. It was heated by a thermal resistor to 78 °C, giving a vapor density of $N=1.0\times 10^{18}$ m^{-3}. The cell was mounted on a translation stage moved by a computer-controlled stepper motor, and was scanned through roughly 200 mm along the focused beam through the beam waist. We recorded the transmission through the aperture at each z position, producing z-scan curves.

In Fig. 1, we have typical z scans for the region to the blue of the ^{85}Rb $F=3\rightarrow F'$ transition with: (a) $\delta=0.8$ GHz, input power 1.0 mW; (b) $\delta=1.1$ GHz, input power 5.0 mW. In Fig. 2, we have typical scans for the region to the red of the ^{87}Rb $F=2\rightarrow F'$ transition with: (a) $\delta=0.9$ GHz, input power 6.0 mW; (b) $\delta=1.1$ GHz, input power 8.0 mW.

In order to reduce statistical noise we took each scan four times and averaged the results. Even after this averaging there was systematic noise in the scans at the level of $\pm 1\%$ of full transmission, which resulted from residual fringing (interference) effects in the Rb cell. Fortunately, the primary fringe in our scan occurred in the wing where the transmission is nearly unity, and so did not badly interfere with our fits, which are mostly sensitive to the behavior of the scan near the beam waist. An interesting side note is that this fringe has a nonlinear phase contribution, since it becomes

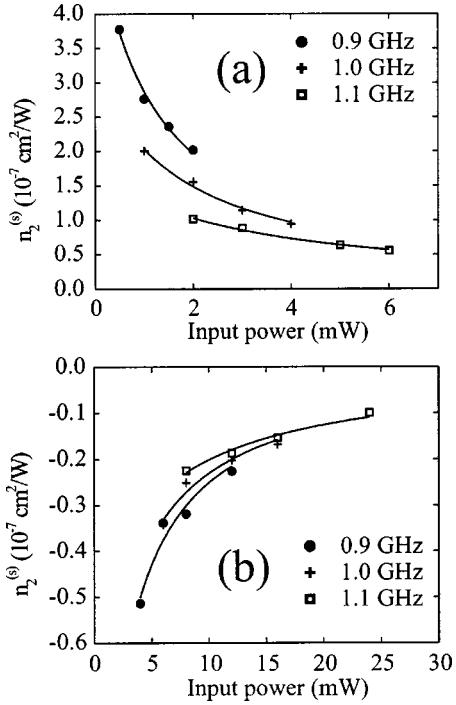

FIG. 3. Saturation fit for the saturated Kerr coefficient $n_2^{(s)}$. (a) Blue detunings from the ^{85}Rb $F=3\rightarrow F'$ transition; (b) red detunings from the ^{87}Rb $F=2\rightarrow F'$ transition.

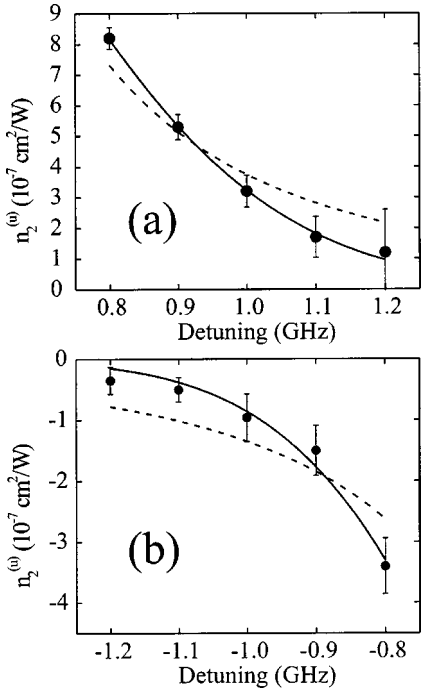

FIG. 4. Kerr coefficient n_2 for the $D2$ line of rubidium vapor. (a) Blue detuning from the ^{85}Rb $F=3\rightarrow F'$ transition; (b) red detuning from the ^{87}Rb $F=2\rightarrow F'$ transition. The dashed line is a fit to Eq. (1) and the solid line is a fit to Eq. (2).

more pronounced at higher intensities (compare the region around the 100 mm position in Figs. 1 and 2).

For purely Kerr media, the z-scan data with a thin sample can be fit to a simple curve, which is derived using the Gaussian decomposition method [15]. In the limit of a low-fluency aperture and a small on-axis nonlinear phase shift ($\Delta\phi_0 \ll \pi$), the theoretical transmission curve is given by [12]

$$T(y) = 1 + \frac{4y\Delta\phi_0}{(1+y^2)(9+y^2)}, \tag{3}$$

where $\Delta\phi_0$ is the on-axis nonlinear phase change induced by the medium at the beamwaist and $y \equiv z/z_R$. The value of n_2 is then calculated using the simple expression $n_2 = \Delta\phi_0/kLI_0$, where I_0 is the intensity at $r=z=0$.

The results of a z scan are more difficult to interpret when the nonlinearity is not purely Kerr, since the perturbative Gaussian decomposition approach is not simple to apply and no analytic solution is known. Various authors have approached this problem numerically [16,17], and typically the correction is small within an order of magnitude of the saturation intensity.

The systematic (fringe) noise in our experiment required us to use intensities at or slightly above the saturation intensity for many of our z scans. In this weakly saturated regime, fitting the experimental data to the curve given in Eq. (3) produces a maximum error of a few percent. This small deviation suggests that a perturbative modification of this equation is plausible for weak saturation. To first order in the perturbation, the Rayleigh range in Eq. (3) becomes a fit parameter. This approach produced reasonable agreement with the data. The fit values of the Rayleigh range were generally larger than the estimated 6 mm, clustering around 7 to 9 mm. Using the "saturated" $\Delta\phi_0$ of these fits, we extracted a saturated coefficient $n_2^{(s)}$. For each detuning we took z scans for a variety of input intensities, and found that $n_2^{(s)}$ itself followed a clear saturation law, given by

$$n_2^{(s)} = \frac{n_2^{(u)}}{1 + I_0/I_s}, \tag{4}$$

where $n_2^{(u)}$ is the Kerr coefficient and I_s is the saturation intensity (see Fig. 3).

The results for $n_2^{(u)}$ obtained from the saturation fit using Eq. (4) are shown in Fig. 4 as a function of detuning frequency, and the predicted and measured values at two particular detunings are given in Table I. Since in both the blue- and red-detuned cases only one isotope is generally relevant (^{85}Rb in the blue case and ^{87}Rb in the red case), the number density in the prediction for n_2 has been scaled by the isotopic abundance. Both models come within about 30% of the measured value at these two detunings. Figure 4 also shows fits to the two models. The best-fit homogeneous model matches the data significantly less well than the Doppler-broadened model, although the Doppler model is a two-parameter fit (total amplitude and the Doppler width). For the blue-detuned case, the fit width is 559 MHz while for the red-detuned case it is 478 MHz, both larger than the predicted value of $ku/2\pi = 336$ MHz. Some of this discrepancy may be due to the hyperfine structure of the transition, which serves to increase the effective Doppler width from the

TABLE I. Comparison of $n_2^{(u)}$ at ± 1.0 GHz detuning, in units of 10^{-7} cm^2/W; data and two theoretical models. The inhomogeneous model uses $ku = 2\pi \times 336$ MHz.

Detuning	Data	Homogeneous model	Inhomogeneous model
+1.0 GHz	+1.6	+2.1	+2.2
−1.0 GHz	−1.0	−0.8	−0.9

simple two-level value. The remainder may be partly due to the presence of the other isotope. It is clear, however, that the inhomogeneous functional form more closely matches the measured values, indicating that even at detunings of several times the Doppler width the simple inverse-cubic model is not sufficient to closely predict values of n_2. It is worth noting that under the Doppler model the nonlinear coefficient falls off exponentially rather than polynomially at large detunings. This reduces the range of "useful" detunings for which absorption is negligible but n_2 is relatively large.

The large value and tunability of the Kerr coefficient n_2 in atomic rubidium makes it an attractive candidate for a variety of nonlinear optical experiments. We have measured n_2 at various detunings on both sides of the $D2$ line of atomic rubidium, finding values of $\sim \pm 10^{-7}$ cm^2/W for ~ 1 GHz detunings around $D2$ line. Saturation effects complicate the results of our z scan data, but they can be adequately dealt with by a simple saturation model. The frequency dependence of n_2 more closely follows the functional form of an inhomogeneously broadened two-level system than a simple far-off-resonance homogeneously broadened two-level transition, although this model remains imperfect.

This work was supported by NSF Grant No. 0101501 and ONR. J.M.H. is grateful for the support from Instituto do Milênio de Informação Quântica, CAPES, CNPq, FAPEAL, PRONEX-NEON, ANP-CTPETRO.

[1] D. Grischkowsky, Phys. Rev. Lett. **24**, 866 (1970).
[2] J.E. Bjorkholm and A. Ashkin, Phys. Rev. Lett. **32**, 129 (1974).
[3] G.A.S. Swartzlander, Jr., H. Yin, and A.E. Kaplan, Opt. Lett. **13**, 1011 (1988).
[4] B. Ai *et al.*, Appl. Phys. Lett. **64**, 951 (1993).
[5] A.G. Truscott *et al.*, Phys. Rev. Lett. **82**, 1438 (1999).
[6] R. Kapoor and G.S. Agarwal, Phys. Rev. A **61**, 053818 (2000).
[7] D.H. Close, Phys. Rev. **153**, 360 (1967).
[8] C.F. McCormick *et al.*, J. Opt. Soc. Am. B **20**, 2480 (2003).
[9] R.H. Lehmberg, J. Reintjes, and R.C. Eckardt, Phys. Rev. A **13**, 1095 (1976).
[10] S. Sinha *et al.*, Opt. Lett. **203**, 427 (2002).
[11] M. Sheik-Bahae, A.A. Said, and E.W.V. Stryland, Opt. Lett. **14**, 955 (1989).
[12] M. Sheik-Bahae *et al.*, IEEE J. Quantum Electron. **QE-26**, 760 (1990).
[13] P.N. Butcher and D. Cotter, *The Elements of Nonlinear Optics* (Cambridge University Press, Cambridge, 1990).
[14] J.A. Andersen *et al.*, Phys. Rev. A **63**, 023820 (2001).
[15] D. Weaire *et al.*, Opt. Lett. **4**, 331 (1979).
[16] L.C. Oliveira, T. Catunda, and S.C. Zilio, Jpn. J. Appl. Phys., Part 1 **35**, 2649 (1996).
[17] T. Hashimoto *et al.*, J. Appl. Phys. **90**, 533 (2001).